Published online 22 September 2013 *Nucleic Acids Research, 2014, Vol. 42, No. 1* ***599–608***
doi:10.1093/nar/gkt846

Independent parallel functions of p19 plant viral suppressor of RNA silencing required for effective suppressor activity

Éva Várallyay, Enikő Oláh and Zoltán Havelda*

Agricultural Biotechnology Center, Institute for Plant Biotechnology, Plant Developmental Biology Group, Szent-Györgyi A. út 4, Gödöllő H-2100, Hungary

Received May 31, 2013; Revised August 9, 2013; Accepted August 30, 2013

ABSTRACT

Plant viruses ubiquitously mediate the induction of miR168 trough the activities of viral suppressors of RNA silencing (VSRs) controlling the accumulation of ARGONAUTE1 (AGO1), one of the main components of RNA silencing based host defence system. Here we used a mutant Tombusvirus p19 VSR (p19-3M) disabled in its main suppressor function, small interfering RNA (siRNA) binding, to investigate the biological role of VSR-mediated miR168 induction. Infection with the mutant virus carrying p19-3M VSR resulted in suppressed recovery phenotype despite the presence of free virus specific siRNAs. Analysis of the infected plants revealed that the mutant p19-3M VSR is able to induce miR168 level controlling the accumulation of the antiviral AGO1, and this activity is associated with the enhanced accumulation of viral RNAs. Moreover, saturation of the siRNA-binding capacity of p19 VSR mediated by defective interfering RNAs did not influence the miR168-inducing activity. Our data indicate that p19 VSR possesses two independent silencing suppressor functions, viral siRNA binding and the miR168-mediated AGO1 control, both of which are required to efficiently cope with the RNA-silencing based host defence. This finding suggests that p19 VSR protein evolved independent parallel capacities to block the host defence at multiple levels.

INTRODUCTION

RNA silencing is a small RNA-based regulatory system that controls target RNAs by endonucleotic cleavage or translational repression through the activities of ARGONAUTE (AGO) proteins (1,2). Plant virus infections are associated with the accumulation of virus-specific small interfering RNAs (siRNAs) generated by the activity of Dicer-like proteins, which are then incorporated into the AGO protein containing RNA-induced silencing complex (RISC) bringing about the sequence specific degradation of viral RNAs (3). To evade the siRNA-based antiviral host defence plant viruses have evolved viral suppressors of RNA silencing (VSRs) interfering with the RNA-silencing pathway mainly by sequestering viral siRNAs or interacting with key RNA silencing components (4,5). Micro RNAs (miRNAs) represent another RNA-silencing pathway, which are indispensable for the control of wide variety of biological functions, including development, hormone responses, feed-back mechanisms, biotic and abiotic stresses (2). miRNAs are generated by sequential processing of genome-coded long single-stranded RNA. AGO1 is one of the most important AGO proteins playing central role in miRNA-mediated regulation of endogenous mRNAs and siRNA-directed control of virus infections (6). *AGO1* mRNA itself is a subject of an miRNA-mediated regulation via the activity of miR168 (7–9). Plant virus infections are often associated with increased miR168 level leading to the downregulation of the antiviral AGO1 (10). Tombusvirus p19 VSR was shown to be responsible for over-accumulation of miR168, which resulted in downregulation of AGO1 protein level (10). Previously, it was demonstrated that the main activity of p19 VSR is to bind selectively and hence sequester viral specific siRNAs (11,12). Recently, it was found that other unrelated VSRs are responsible for miR168 induction and the subsequent AGO1 level control (13). This observation indicates that miR168-mediated alleviation of RNA silencing-based host defence might be a widespread viral counter defence mechanism. However, it remained to be elusive whether miR168 induction is the consequence of the main suppressor activity of VSRs or it is an independently evolved parallel function. All of the investigated VSRs possessing the ability to induce the miR168 level

*To whom correspondence should be addressed. Tel: +36 28526155; Fax: +36 28526101; Email: havelda@abc.hu

show certain RNA-binding capacities (13). This raised the possibility that the RNA binding may be critical for induction of miR168 level.

In this work, we demonstrate that the ability of p19 VSR to induce the accumulation of miR168 is not connected to its ability to bind virus specific siRNAs. We show that the presence of a siRNA binding deficient p19 VSR in the infection process is associated with the induction of miR168 level and the subsequent control the AGO1 accumulation. The efficient miR168 driven control of AGO1 by siRNA-binding deficient p19 VSR results in higher virus titer and the development of more sever disease symptoms indicating the biological relevance of this regulatory process. These data indicate that the control of AGO1 protein level is an important component of the efficient tombusvirus invasion. Moreover, our data suggest that siRNA binding and mir168 inducing capacities of p19 VSR evolved independently providing a multiple parallel counter defence activities to suppress RNA silencing successfully.

MATERIALS AND METHODS

Plant materials, viruses

Nicotiana benthamiana was used as systemic host. Plants were grown in soil under normal growth conditions and were infected by wild-type carnation Italian ringspot virus (CIRV) or mutant viruses by mechanical inoculation using *in vitro* RNA transcripts as described previously (14). Virus infected plants were grown in fitotron at 21 or 15°C.

Construction of CIRV-3M mutant virus and infectious clones

Site-directed mutagenesis of p19 (p19-3M) was carried out by PCR using the p19-coding region (between 3872 and 4390 nt) of the CIRV genome (15) cloned in pUC18 and then confirmed by DNA sequencing. We used CIRVp19E41Vs:aaacttcctgacgaaagtccgagtgggactgtcgggcggctatataac and CIRVp19E41Vrevcomplas: gttatatagcc gcccgacagtcccactcggactttcgtcaggaagttt megaprimers and CIRVp19E41Vs:gtgggactgtcgggcggctatataac CIRVp19E41 Vrevcomplas:gttatatagccgcccgacagtcccac oligonucleotides for the PCR mutagenesis. The p19-3M coding region has been introduced into the clone of full-length CIRV genomic RNA-generating functional p19-3M expressing mutant virus (CIRV-3M). The modifications of CIRV-3M did not alter the amino acid sequence of the p22 movement protein encoded by ORF4.

Protein expression and electrophoretic mobility shift assay

CIRV p19 and p19-3M VSRs were expressed and purified as a GST fusion protein in *Escherichia coli* strain BL21(DE3) at 22°C for 20 h according to the manufacturers' instruction (GE Healthcare Life Sciences). Briefly, bacterial pellets were resuspended, and the fusion protein was purified from the soluble fraction of lysate by batch method incubating with glutathione agarose resin for 30 min at 21°C. The resin was washed four times with cleavage buffer [0.05 M Tris–HCl, 0.15 M NaCl, 0.005 M MgCl2, 1 M DTT, 0.02% Tween-20 (pH 7.4)]. The resin was incubated with thrombin (Amersham Biosciences) for 3 h at room temperature. After cleavage, the liberated p19 protein was collected. Synthetic radiolabelled siRNA was produced as described previously (16). The sequences of the RNA oligonucleotides used are 5′ UGAUAUUGGCA CGGCUCAAUC 3′ and 3′ UUGAGCCGUGCCAAUA UCAUC 5′. Direct binding experiment of CIRV p19 and p19-3M was carried out as described previously (17). Purified p19 and p19-3M protein VSRs (3 nM) were added to 1 pM radiolabelled siRNA in binding buffer [containing 0.05 M Tris–HCl, 0.15 M NaCl, 0.005 M $MgCl_2$, 0.02% Tween-20, (pH 7.0)]. Binding reactions were incubated at 25°C for 30 min, complemented with 3 µl of loading dye, and the reaction was analyzed by electrophoresis at a constant 50 V for 1.5 h through a 6% TBE DNA retardation gel in 0.5X TBE. The gels were then dried then exposed.

RNA isolation and northern blotting

Total RNA was extracted from virus infected plants displaying symptomatic systemically infected or from infiltrated leaves. In all, 0.1 g of homogenized plant material were resuspended in 400 µl of extraction buffer [0.1 M glycine–NaOH (pH 9.0), 100 mM NaCl, 10 mM EDTA, 2% sodium dodecyl sulfate and 1% sodium lauroylsarcosine] and divided into two aliquots. In all, 300 µl of extra extraction buffer was added to 300 µl of this extract and mixed with an equal volume of phenol. The other part was used for protein extraction. The aqueous phase was treated with an equal volume of phenol chloroform. For northern blot analyses of mRNAs, 8–10 µg of total RNA was separated on formaldehyde-1.2% agarose gels and blotted to Nytran NX membrane (Schleicher & Schuell, Germany). PCR products were used for producing radioactively labelled random priming probes by Decalabel DNA labelling kit (Fermentas) detecting endogenous mRNAs. Membranes were hybridized using the Perfect Hyb buffer (Sigma) according to manufacturer's instruction. For small RNA northern blot analyses (18), the total RNA samples (8–10 µg) were fractionated on denaturing 12% polyacrylamide gels containing 8 M urea, transferred to Nytran N membrane (Schleicher & Schuell, Germany) by capillary method and fixed by ultraviolet cross-linking. Membranes were probed with radioactively labelled LNA oligonucleotide probes (Exiqon, Denmark), complementary to the mature microRNAs. In all, 5 pmol of each oligonucleotide probe was end-labelled with [γ32P]ATP by using T4 polynucleotide kinase. Prehybridization of the filters was carried out in 50% formamide, 0.5% SDS, 5xSSPE, 5xDenhardt's solution and 20 µg/ml sheared, denatured, salmon sperm DNA. The hybridization was carried out at 50°C for 2 h in the same buffer. Washing of the membranes was done for 10 min two times with washing solution containing 0.1% SDS and 2xSSC at the temperature of the hybridization.

CIRV-specific small RNA fraction was detected with minus strand-specific RNA probe, what was transcribed form the cloned positive strand virus with T7 RNA

polymerase in the presence of radioactive UTP. The small RNA northern blot analysis for virus-specific siRNAs was carried out at 37°C for 16 h.

Western blot analysis

For protein analyses, 0.1 g of plant material was collected (from systemically virus infected or agroinfiltrated leaves) and homogenized in an ice cold mortar in 400 µl of extraction buffer [0.1 M glycine-NaOH (pH 9.0), 100 mM NaCl, 10 mM EDTA, 2% sodium dodecyl sulfate and 1% sodium lauroylsarcosine]. In all, 100 µl of 2X Laemmli buffer was added to 100 µl of the homogenized sample and used for protein analysis. The remaining sample was complemented with 300 µl of extraction buffer and further processed for RNA extraction. This method ensures the comparability of protein and RNA samples. Protein samples were treated as described previously (19) and 20–30 µl of sample was resolved on 8% sodium dodecyl sulfate–polyacrylamide gel electrophoresis, blotted to PVDF Transfer Membrane (Amersham Hybond-P) and subjected to western blot analysis. Membranes were blocked using 5% non-fat dry milk in PBS containing 0.05% Tween 20 (PBST) for 30 min. The target proteins were detected using anti *N. benthamiana* AGO1-1 (1:250; the custom antibody against *N. benthamiana* AGO1-1 protein) (10) and anti-p19 (17). We hybridized the membranes with the antibodies in PBST or in PBST 2.5% non-fat dry milk (AGO1-1 antibody) at room temperature for 1–2 h. After washing the membranes in PBST, secondary peroxidase-conjugated anti-rabbit was added. The signals were visualized by chemiluminescence (ECL kit; Amersham) according to the manufacturer's instructions. The membranes were stained with Ponceau stain for checking protein loading.

Analysis of hybridization results

Quantitative analysis of hybridization results were done by ImageQuant 5.2 software.

Gel filtration assay

Crude protein extracts were prepared from systemic, virus infected or from mock-inoculated leaves and fractionated on a Superdex-200 gel filtration column as described previously (10). In all, 0.4 g of leaf tissue was homogenized in 800 µl of ice-cold RISC buffer (100 mM KAc, 5 mM MgAc, 4 mM DTT, 40 mM HEPES: pH7.5) and centrifuged twice for 5 min at 4°C at full speed. The supernatant was filtered through a 0.22 µm filter (Millipore), and 200 µl of the clear supernatant was loaded onto a RISC buffer equilibrated Superdex-200 (Pharmacia) column. The sample was size separated at 0.25 ml/minute flow rate at 4°C using a FPLC (Pharmacia) system. Approximately 300 µl of fractions were taken. The first 20 fractions were discarded and the following 48 fractions were collected. Odd number fractions were used for RNA while even number fractions were used for protein extractions. For RNA extraction, 300 µl of equal volumes of phenol and chloroform was added to each fraction, precipitated with ethanol and resuspended in 10 µl of sterile water and used for small RNA northern blotting. The RNA blot was hybridized with CIRV minus strand-specific RNA probe detecting viral siRNAs. To investigate p19 accumulation 1200 µl of cold acetone was added to each fraction, left at 20°C to precipitate, centrifuged, washed with 70% EtOH, dried and resuspended in 10 µl of 2X Laemmli buffer and used for western blot analyses. The elution positions of protein molecular markers are as follows: 158 kDa, aldolase; 66 kDa, bovine serum albumin; 29 kDa, carbonic anhydrase.

Immunoprecipitation

For immunoprecipitation (IP) systemically infected leaves of CIRV, CIRV19Stop, CIRV-3M and mock inoculated *N. benthamiana* plants were collected at 6 days postinoculation and used to prepare extracts (1 g of plant material in buffer containing [100 mM KAc, 5 mM MgAc, 4 mM DTT, 40 mM HEPES (pH7.5) and Proteinase inhibitor (Sigma, P9599)]. P19 antibody was added to the crude extracts, and IP reactions were carried out at 4°C for 3 h, and then Sepharose A CL-4B beads were centrifuged and washed five times. Input extracts and eluates of IPs were used for protein and RNA isolation.

RESULTS

The p19-3M mutant is deficient in siRNA-binding activity

Tombusvirus p19 VSRs were shown to mediate silencing suppression mainly by highly specific binding and hence sequestering viral-specific siRNAs (11,12). Trp39 and Trp42 of p19 VSR are the key residues responsible to form stacking interactions with siRNAs by capping the exposed RNA base pairs at each end of the duplex (17,20). The CIRV p19 VSR showed high affinity for synthetic siRNA duplexes in gel mobility shift assay (17). We produced the CIRV W39G-W42G-E41V p19 mutant (p19-3M), which contains glycine to tryptophan substitutions in the 39 and 42 positions resulting in no stacking interaction of both side chains with siRNAs. Because of the overlapping viral ORFs, these modifications also caused a serine to arginine change at position 53 of the p22 movement protein, encoded by ORF4 (14). To restore this position back to serine, a third mutation (E41V) was introduced rendering these mutations silent in p22 movement protein. To analyze the siRNA-binding ability of p19-3M, we expressed the mutant protein and investigated its affinity for synthetic siRNA duplexes in gel mobility shift assay in comparison with the wild-type p19 VSR (Figure 1). We found that although the wild-type p19 VSR showed extremely high affinity to labelled siRNAs p19-3M lost its siRNA-binding ability showing no any residual binding activity. These data show that multiple mutations in the siRNA-binding territories render p19 VSR completely deficient in siRNA binding in *in vitro* analysis.

Viral expression of p19-3M results in the accumulation of unbound virus-specific siRNAs

First, we confirmed the lack of siRNA-binding ability of p19-3M mutant *in vivo* by preparing crude extracts from

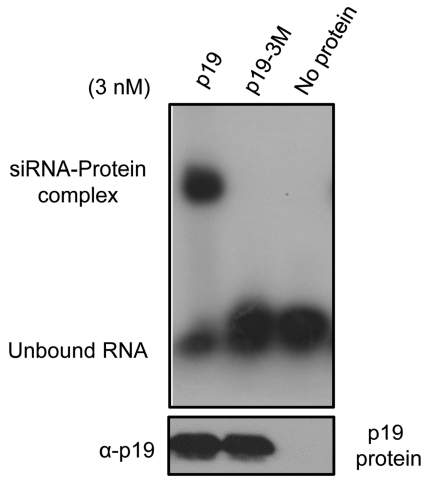

Figure 1. p19-3M does not bind viral siRNAs. Wild-type p19 and p19-3M VSRs were expressed in bacterial expression system and use for gel mobility shift assay performed with 21mer synthetic siRNA with 2 nt, 3′ overhangs and 5′ phosphate groups (upper panel). The synthetic siRNA (1 pM concentration) was added to p19 or p19-3M VSRs at 3 nM protein concentration and separated on 6% native acrylamide PAGE. The presence and quality of the expressed proteins were confirmed by western blot analyses using p19 specific antibody (α-p19; bottom panel).

CIRV, CIRV19Stop (p19 deficient mutant) and CIRV-3M (mutant virus carrying p19-3M) infected *N. benthamiana* plants for IPs using p19-specific antiserum. Our western and northern blot analyses showed that only precipitate of crude extract from wild-type CIRV infection contained viral siRNAs, and they were not present in CIRV-3M precipitate (Figure 2A). In accordance with gel mobility shift assay data, our results confirmed that p19-3M has lost its efficient siRNA-binding capability in the infected plants.

Using a gel filtration approach, it was demonstrated that in Tombusvirus-infected plants, the majority of viral-derived siRNAs were bound by the p19 VSR, whereas in the absence of p19, the viral siRNAs accumulated in fractions corresponding to the size of unbound (free) siRNAs (10,12). We used the same experimental approach to test how p19-3M interferes with the accumulation of viral-derived siRNAs in virus infected plants. We also used a previously described single mutant possessing only a glycine to tryptophan substitution in the 39 position of the CIRV p19 VSR (p19-1M) (17). Crude extracts of CIRV, CIRV19Stop, CIRV-1M (mutant virus carrying p19-1M), CIRV-3M and mock inoculated *N. benthamiana* plants were loaded on gel filtration column, and the ratio of p19 bound siRNA was investigated relative to the free siRNAs as described previously (10). In CIRV-infected plants, fractions 27 and 29 contained the majority of viral siRNAs, which are p19 bound (Figure 2B). In contrast, in the case of CIRV19Stop, unbound viral siRNAs occupy fractions 33–37. Analyses of a crude extracts derived from CIRV-1M indicated that this mutant retained a partial siRNA-binding capacity (Figure 2B). These data are in accordance with previous results demonstrating that a similar p19 mutant also retained residual siRNA-binding ability (21). However, analyses of the crude extract derived from CIRV-3M infection demonstrated that the p19-3M mutant

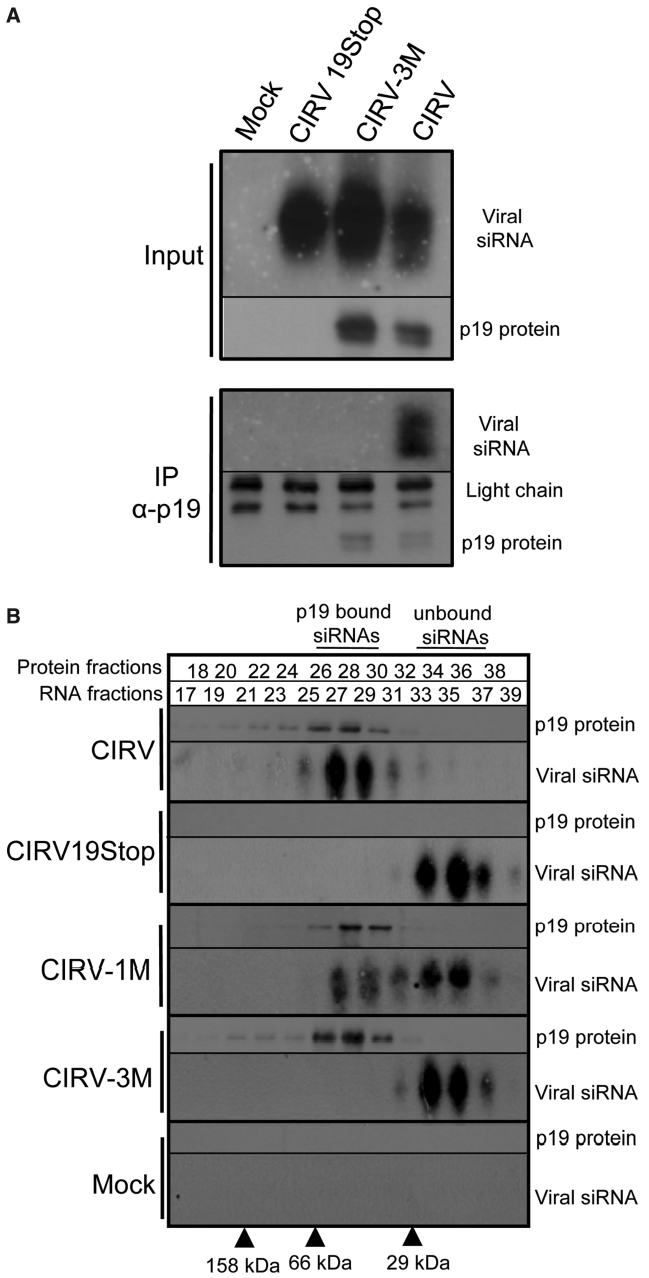

Figure 2. CIRV-3M infection is associated with accumulation of unbound siRNAs. (**A**) IP of viral siRNAs using p19-specific antibody (α-p19) on crude protein extracts of CIRV-, CIRV19Stop-, CIRV-3M- and mock-inoculated plants. The input and the IP were probed for viral-specific siRNAs and for the presence of p19. (**B**) Gel filtration of crude extracts prepared from systemically infected leaves (6 dpi.) of CIRV-, CIRV19Stop-, CIRV-3M- and mock-inoculated plants. Even number fractions were used for p19 western blot analyses, whereas odd number fractions were used for small RNA northern blotting. Fractions were separated on small RNA polyacrylamide gel, blotted and hybridized with virus-specific positive sense RNA probe to detect virus derived negative sense siRNAs. Fractions 27 and 29 represent p19 bound siRNAs, fractions 33, 35 and 37 accumulate free virus-specific siRNAs.

protein, although expressed at high level, lost its ability to bind viral siRNAs. In this case, viral-specific siRNAs accumulated in fractions 33–37, corresponding to free siRNAs, and no virus-specific siRNAs were present in

27–29 fractions, where normally p19 bound siRNAs were observed. These data demonstrate that the recombinant virus, CIRV-3M, can mediate the stabile expression of p19-3M, which is not able to bind siRNAs resulting in the exclusive accumulation of unbound siRNAs.

Viral expression of p19-1M and p19-3M induces miR168 over accumulation

Next, we tested the potential of p19-1M and p19-3M in interfering with the accumulation of AGO1 during the virus infection process. *Nicotiana benthamiana* test plants were inoculated with CIRV, CIRV19Stop, CIRV-1M or CIRV-3M at 21°C and sampled when systemic symptoms appeared. RNA and protein was extracted from the apical systemically infected leaves and the levels of *AGO1* mRNA, AGO1 protein and miR168 were determined. In line with our previous observations (10), we have detected the efficient induction of *AGO1* mRNA in CIRV and CIRV19Stop-infected plants at 21°C, which was also a characteristic for CIRV-1M and CIRV-3M-inoculated plants (Figure 3A and B). Similarly, as already demonstrated for cymbidium ringspot virus, the AGO1 protein level did not show enhanced accumulation in wild-type CIRV-infected plants because of the inhibitory activity resulting from the increased miR168 level. In contrast, in the absence of p19 (CIRV19Stop), no induction of miR168 can be detected and consequently the AGO1 protein level is significantly upregulated (Figure 3A and B). However, we observed that infection with CIRV-1M or CIRV-3M was associated with the induction of miR168 and the suppression of AGO1 protein level (Figure 3A and B). At 21°C, siRNA-mediated RNA-silencing works efficiently inhibiting the mutant virus, lacking fully functional p19 VSR, to accumulate to higher level. As at 15°C this process in inhibited (22), we tested our experimental system at this temperature to reach higher virus titer in the p19-3 M VSR mutant infection. We took samples from the symptomatic systemically infected leaves at 16 dpi., as the symptom development is slower at this temperature, and observed the induction of miR168 and subsequent AGO1 level control by CIRV-3M (Figure 3C). In CIRV-3M infection reduced level of virus was present resulting in lower level of miR168 induction compared with the wild-type CIRV infection. The level of miR168 induction can be proportional with the amount of the virus, as the induction of miR168 spatially overlaps with the virus accumulation in the infected tissue (Varallyay *et al.* 2010). As the viral RNA levels do not correlate with the AGO1 protein accumulation at the investigated time points, we tested whether the levels of viral siRNAs generated by mutant viruses are sufficient to load AGO1 protein. We found that the relative accumulation of viral siRNAs in CIRV19Stop, CIRV-1M and CIRV-3M infections was even enhanced compared with the wild-type infection. AGO2 plays an important antiviral role in *N. benthamiana* (23), and it has been shown, using AGO2 specific antibody, that AGO2 protein over-accumulates in Tombusvirus-infected plants (V. Tisza and J. Burgyán, unpublished result). Therefore, we tested AGO2 protein accumulation in our system and

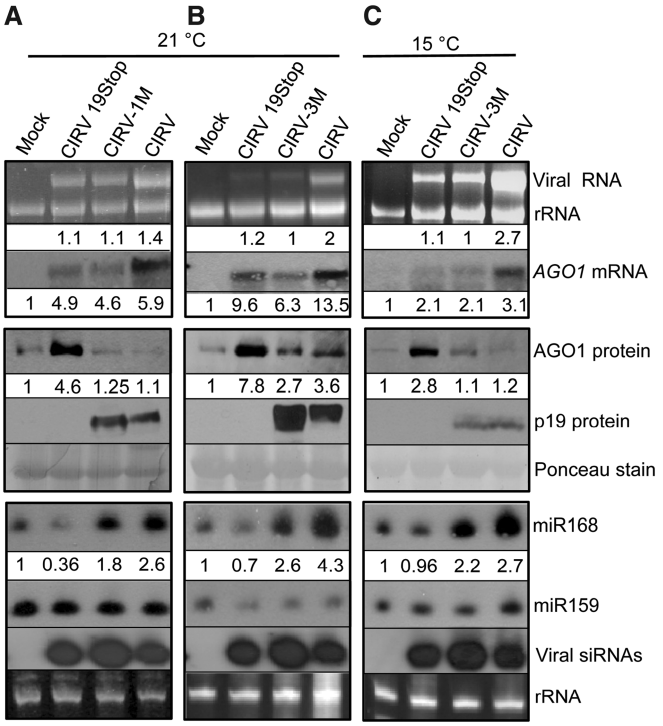

Figure 3. Viral expression of p19-1M and p19-3M induces miR168 over accumulation. Systemically infected leaves of CIRV-1M at 21°C at 6 dpi. (**A**), CIRV-3M at 21°C at 5 dpi. (**B**) CIRV-3M at 15°C 16 dpi. (**C**) and the corresponding CIRV19Stop, CIRV and mock inoculated *N. benthamiana* plants were homogenized and divided into RNA and protein extractions. The corresponding samples were used for detecting *AGO1* mRNA, AGO1 protein and miR168 expressions. Top panels: Northern blot analyses of virus infected and mock inoculated plants for *AGO1* mRNA. Ethidium bromide-stained agarose gel was used as loading control. Numbers show the relative viral RNA and *AGO1* mRNA levels normalized to rRNA intensity. Middle panels: Western blot analyses of total protein extracts for AGO1 and p19 protein accumulation. Ponceau staining of the membrane served as loading control. Numbers show the relative AGO1 protein levels normalized to Ponceau staining. Bottom panels: Small RNA northern blot analyses using miR168- and miR159-specific LNA probes and virus-specific RNA probe. Relative gel loadings are also indicated by ethidium bromide staining of ribosomal RNA. Numbers show the relative miR168 levels normalized to rRNA intensity.

found that all virus infections were associated with enhanced accumulation of AGO2 (Supplementary Figure S1), indicating that this protein can take over the function of AGO1.

Altogether, these data indicate that partial or full inhibition of the siRNA-binding ability of p19 VSR does not influence its capacity to enhance the level of miR168 implying that these two properties of p19 VSR is independent.

P19-3M-mediated control of AGO1 influences the development of virus induced symptoms

The biological relevance of p19-mediated miR168 driven AGO1 control in the virus infection process was investigated by comparison of CIRV-3M and CIRV19Stop virus infections. CIRV-3M is expressing the completely siRNA-binding deficient p19-3M, which retained its ability to

induce miR168 level and control AGO1 accumulation while CIRV19Stop lost both p19-related functions. Tombusvirus infection leads to extremely high-level accumulation of viral RNAs (Figure 4A) and the subsequent necrosis of the systemically infected leaves of *N. benthamiana* by 8–10 dpi., which eventually culminates in the death of the plant (17,24). In contrast, the loss of p19 VSR mutant virus (CIRV19Stop) inoculated plants exhibit RNA silencing associated recovery phenotype and have markedly reduced virus titer (21,25,26). Infections with a Tombusvirus carrying a single p19 mutation were shown to be associated with development of the recovery phenotype (17,21). *Nicotiana benthamiana* test plants were infected with wild-type CIRV, CIRV19Stop and CIRV-3M, and the developing symptoms were monitored. We expected a more efficient replication of CIRV-3M relative to CIRV19Stop infection because of the miR168 driven inhibitory effect of p19-3M on the over accumulation of AGO1 containing antiviral RISCes. In agreement with this hypothesis, investigation of RNA samples extracted from the infected plants at 10 dpi. revealed that CIRV-3M replicated more efficiently than CIRV19Stop where the over-accumulation of antiviral RISCes was not blocked (Figure 4A). We found that CIRV19Stop and also CIRV-3M infections result in development of the recovery phenotype while the wild-type virus infection is associated with apical necrosis and the death of the plant. However, over a longer time course (16 dpi.) observations revealed that recovery of CIRV-3M infected plants is considerably suppressed, the size of the recovered plants were about the two-third of the size of the recovered plants form CIRV19Stop infection (Figure 4B). These data suggest that although p19-3M has lost its ability to block the accumulation of free viral siRNAs, it is still able to influence the development of viral disease symptoms by modulating the AGO1 level.

P19 VSR-mediated miR168 induction is not affected by the presence of defective interfering RNAs

Tombusvirus-associated defective interfering (DI) RNAs are deletion mutants of the viral genome harnessing the replication system of the parental virus (27). The presence of DI RNAs in the infection process results in suppressed accumulation of the parental genome and in the appearance of recovery like symptoms similar to that of characteristic for p19 (e.g. CIRV19Stop) deficient tombusvirus infections. It was demonstrated that the presence of DI RNAs in viral infections enhances the level of virus-specific siRNAs resulting in the saturation of binding capacity of p19 VSR and the accumulation of unbound siRNAs inducing the RNA silencing associated recovery phenotype (28). We tested whether this specific DI RNA-mediated inhibition of p19 VSR affects its ability to induce miR168 and control the accumulation of AGO1. *Nicotiana benthamiana* pants were infected with CIRV, CIRV with DI RNA, CIRV19Stop and CIRV-3M at 21°C and sampled when systemic symptoms appeared. RNA and protein was extracted from the apical systemically infected leaves and the levels of *AGO1* mRNA, AGO1 protein and miR168 were determined. We found that all infections induced *AGO1* mRNA level at 6 dpi.; however, only CIRV19Stop-infected plants showed enhanced AGO1 protein accumulation (Figure 5A). The DI RNA containing CIRV infection was also associated with induced level of miR168 and controlled AGO1 accumulation similarly to CIRV-3M infection. The analyses of viral RNA accumulation at 10 dpi. revealed that DI

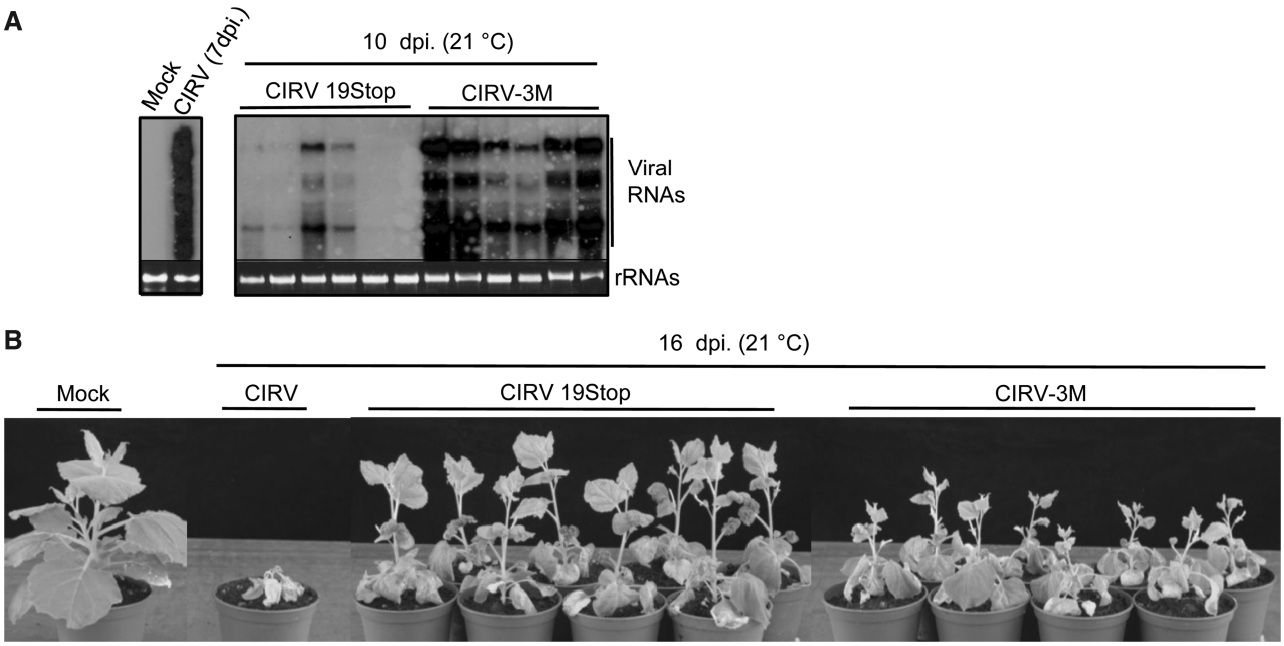

Figure 4. Infection of *N. benthamiana* with CIRV-3M results in enhanced virus accumulation and aggravates symptoms. (**A**) Northern blot detection of virus accumulation in systemically infected leaves of CIRV19Stop and CIRV-3M inoculated *N. benthamiana* plants at 10 dpi. CIRV infection was sampled at 7 dpi. because of the fast necrotic reaction. (**B**) Photos of the *N. benthamiana* plants, mock inoculated or infected with viruses: CIRV19Stop, CIRV-3M and CIRV at 21°C at 16 dpi.

RNA-containing CIRV infection displayed similar replication efficiency of the viral genome as CIRV-3M infection (Figure 5B), and the developing long-term symptoms were also similar to CIRV-3M-induced intermediate severity symptoms (Figure 5C). These data suggest that DI RNA-mediated siRNA saturation driven block of p19 VSR activity does not disturb the induction of miR168, further supporting the hypothesis that these two activities of p19 VSR are independent. Moreover, the development of intermediate severity symptoms in the presence of DI RNAs is associated with the control of AGO1 over accumulation indicating that miR168 induction can be an important component of symptom development also in this case.

DISCUSSION

Infections of different plant viruses induce the activation of RNA silencing-based host defence system, a sequence-specific RNA degradation mechanism, mediated by siRNAs (1,29–31). siRNAs are produced from double-stranded virus-specific RNA species by DICER enzymes and loaded into the AGO protein containing RISCes. Loaded RISCes recognize viral RNAs that have sequence complementary to the loaded siRNA and block their activity by cleavage or by translational inhibition. AGO1 is one of the most important AGO proteins playing central role in miRNA pathway, and its expression itself is regulated by the activity of miR168 (6,9). The central role of AGO1 in the composition of antiviral RISC is supported by observations demonstrating that AGO1 recruits virus-specific siRNAs (32,33) and ago1 hypomorphic mutants are more susceptible to viral infections (34,35). To counteract the efficient RNA silencing-based antiviral mechanism viruses express viral suppressor proteins of RNA silencing (VSR), which are able to disarm the virus infection-induced host defence (5). The increased expression of miR168 and *AGO1* mRNA was observed in different virus-infected plants (10,19,32,36,37). In line with the central role of AGO1 in RNA silencing-based host defence, it was shown that

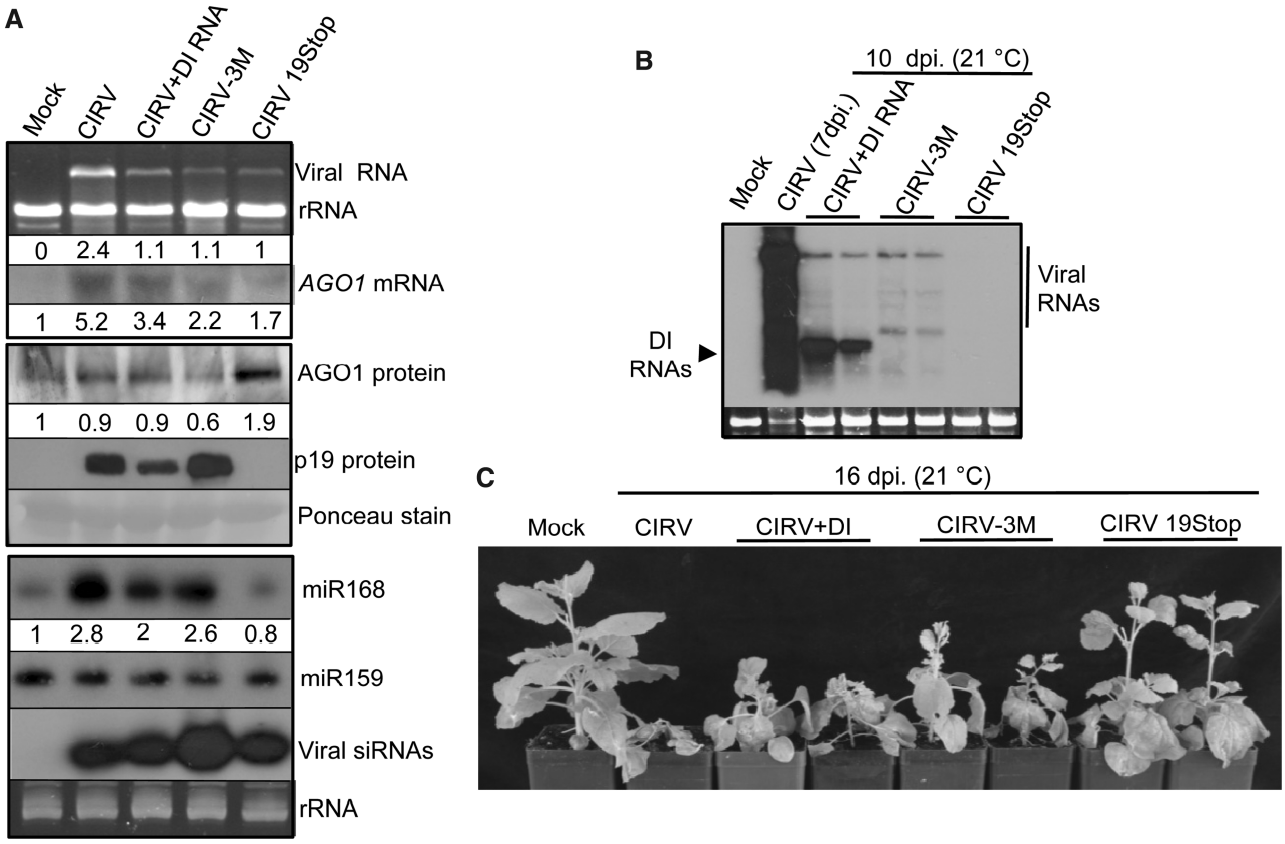

Figure 5. P19 VSR-mediated miR168 induction is not affected by the presence of DI RNAs. (**A**) Systemically infected leaves of CIRV, CIRV with DI RNAs, CIRV-3M, CIRV19Stop virus infected and mock inoculated *N. benthamiana* plants were homogenized and divided into RNA and protein extractions. The corresponding samples were used for detecting *AGO1* mRNA, AGO1 protein and miR168 expressions. Top panels: Northern blot analyses of virus infected and mock inoculated plants for *AGO1* mRNA. Ethidium bromide-stained agarose gel was used as loading control. Numbers show the relative viral RNA and *AGO1* mRNA levels normalized to rRNA intensity. Middle panels: Western blot analyses of total protein extracts for AGO1 and p19 protein accumulation. Ponceau staining of the membrane served as loading control. Numbers show the relative AGO1 protein levels normalized to Ponceau staining. Bottom panels: Small RNA northern blot analyses using miR168- and miR159-specific LNA probes and virus-specific RNA probe. Relative gel loadings are also indicated by ethidium bromide staining of ribosomal RNA. Numbers show the relative miR168 levels normalized to rRNA intensity. (**B**) Northern blot detection of virus accumulation in systemically infected leaves of CIRV with DI RNAs, CIRV-3M, CIRV19Stop inoculated *N. benthamiana* plants at 10 dpi. CIRV infection was sampled at 7 dpi. because of the fast necrotic reaction. (**C**) Photos of the *N. benthamiana* plants, mock inoculated or infected with CIRV, CIRV with DI RNAs, CIRV-3M, CIRV19Stop at 21°C at 16 dpi.

the induction of *AGO1* mRNA expression is a potential host defence mechanism enhancing the concentration of the antiviral RISCes, whereas the virus infection-mediated induction of miR168 and the subsequent control of AGO1 protein accumulation is a viral counter defence strategy (10). Moreover, it was also demonstrated that different unrelated VSRs, in addition to their main silencing suppression function—predominantly siRNA sequestering or interacting with key RNA silencing components—are able to induce the accumulation of miR168 and control the level of AGO1 to alleviate the effect of antiviral RISC on the virus replication (13). These observations suggested a wide-spread viral defence strategy based on AGO1 level control, which raised the questions whether this activity of VSRs are the consequence of their already described main silencing suppression mechanisms or it is an independently evolved parallel activity and is there any biological relevance of this phenomenon in the virus infection process. We used the well-described Tombusvirus system to investigate these questions, as p19 VSR is one of the most intensively investigated plant virus VSRs acting via siRNA sequestering (38). To dissect the two functions, siRNA sequestration and miR168 induction, a siRNA-binding deficient p19 VSR mutant, p19-3M, was constructed, which completely lost its siRNA-binding ability. To understand how p19-3M interferes with the virus infection process and symptom development, a recombinant virus has been produced expressing p19-3M (CIRV-3M), and the infected plants were analyzed for miR168 and AGO1 accumulation. We found that miR168 level was induced in these symptomatic plants, and the AGO1 protein level was kept constant in contrast to the loss-of-p19 mutant (CIRV19Stop) where the complete recovery phenotype was associated with the lack of miR168 induction and immense accumulation of AGO1 protein. A previously described p19 VSR mutant [(17); p19-1M], which only partially lost its siRNA-binding capacity showed similar miR168 driven AGO1 control activity as p19-3M or wild-type p19 VSR indicating that there is no connection between the siRNA-binding efficiency and miR168-inducing capacity of p19 VSR. Our data are in good agreement with previous studies revealing that siRNA binding of p19 can also be uncoupled from other p19 functions such as symptom development and host dependent effects on host RNAs and proteins (39). Increase in AGO1 level would result in an excess of antiviral RISC, so in plants where the AGO1 over-accumulation is inhibited, we would expect higher virus titer despite the presence of high level of unbound virus-specific siRNAs. We observed higher levels of viral RNAs in CIRV-3M than in CIRV19Stop-infected plants, which was associated with more severe intermediate symptoms and suppressed recovery phenotype. We also found that disabling the activity of p19 VSR by overloading its binding capacity by DI RNA-mediated over-production of viral siRNAs does not interfere with the induction of miR168 and the suppression of host-mediated induction of AGO1 level. The moderate host response to virus-mediated miR168 driven control of AGO1 can be explained by the recent observation that in *N. benthamiana* AGO2 has acquired the main antiviral function (23). As different VSRs ubiquitously

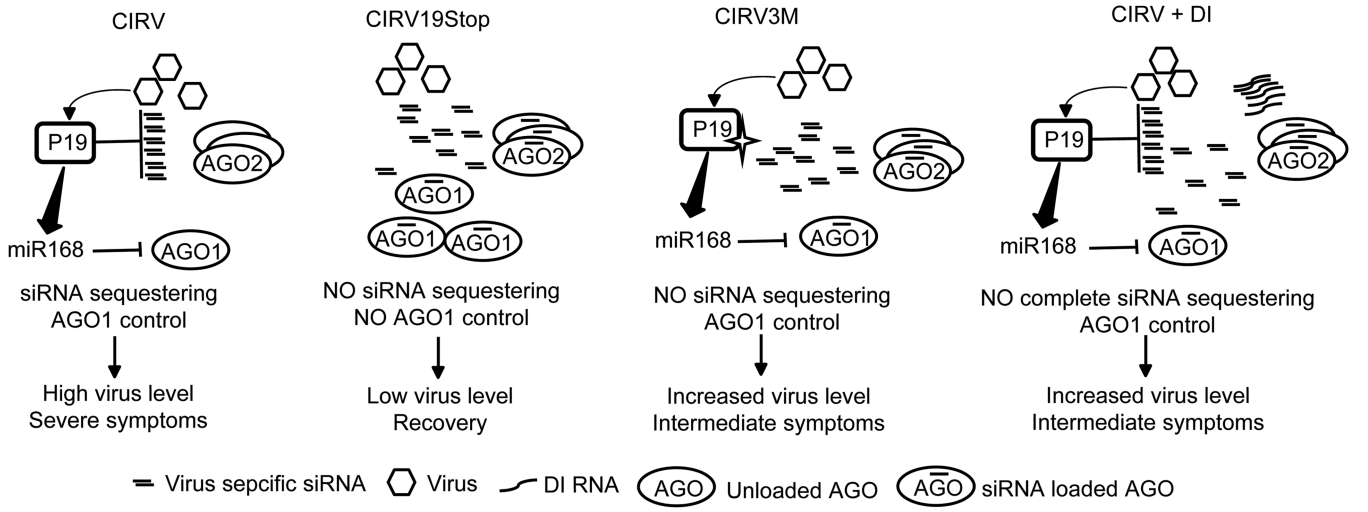

Figure 6. Schematic representation of the proposed model. During CIRV infection, high amount of virus-specific siRNAs are generated and also the *AGO1* mRNA level is induced by the host defence system. In wild-type infection, the p19 VSR is able to bind and thus sequester the generated siRNAs and also enhances the miR168 level resulting in translational control of the antiviral AGO1. In parallel, the antiviral AGO2 level is induced. However, in the lack of free viral siRNAs, AGO proteins remain unloaded. As a result of the efficient suppression strategy, the virus accumulates to high level and induces severe symptoms. If there is no functional p19 VSR in the infection, both of the suppressor activities are absent resulting in over-production of antiviral AGO1 and AGO2 loaded with high amount of virus-specific siRNAs. In this case, the AGO1- and AGO2-mediated host defence successfully limits the virus accumulation and the recovery phenotype develops. In the case of CIRV-3M infection, the binding capacity of p19-3M is disabled resulting in the presence of high amount of unbound siRNAs. However, it is still able to induce the miR168 level and thus limit the accumulation of active siRNA loaded AGO1 containing RISCes. In this case, only AGO2 acts efficiently resulting in higher virus accumulation and more severe symptoms compared to Cym19Stop infection. The similar mechanism takes place when DI RNAs are present in the infected plants. Over-production of viral siRNAs generated from the efficiently replicating DI RNAs overload the binding capacity of p19 VSR. However, despite this inhibition, p19 VSR is able to induce miR168 level and control AGO1 accumulation.

mediate the induction of miR168, it is possible that this activity served as evolutionary driving force to involve other AGO proteins, such as AGO2, in the composition of antiviral RISC in some plant–virus interactions. However, it was shown that miR168 was unaffected in tomato plants infected with turnip crinkle virus, cucumber mosaic virus and tobacco rattle virus (40). In addition, transgenic expression of Tombusvirus p19 VSR in potato had no effect on miR168 level, and no AGO1 control was observed (41). These data indicate that virus-mediated miR168 induction requires host-dependent specific factors.

Altogether, our observation suggests that the capability of miR168 induction was acquired by p19 VSR independently, from its siRNA-sequestering ability and represents a parallel function, which can attack the RNA-silencing pathway at a different point (Figure 6). Moreover, we demonstrate that p19 VSR-mediated miR168 driven control has the capacity to influence the accumulation of the virus in the infected plants and enhance the severity of symptoms indicating that both p19 VSR-mediated independent suppressor activities, siRNA binding and AGO1 control, are necessary to efficiently cope with the host defence system. As many unrelated VSRs are able to modify the miR168 level, it is possible that this phenomenon is an important symptom determinant in other plant-virus interactions as well.

SUPPLEMENTARY DATA

Supplementary Data are available at NAR Online.

ACKNOWLEDGEMENTS

The authors thank György Szittya, József Burgyán and Daniel Silhavy for critical reading and helpful comments on the manuscript. They also thank József Burgyán and György Szittya for providing p19-W39G (p19-1M) mutant and József Burgyán for providing *N. benthamiana* specific AGO2 antibody.

FUNDING

Hungarian Scientific Fund [OTKA K78351 and PD78049]. Funding for open access charge: Hungarian Scientific Fund [OTKA K78351].

Conflict of interest statement. None declared.

REFERENCES

1. Ding,S.W. (2010) RNA-based antiviral immunity. *Nat. Rev. Immunol.*, **10**, 632–644.
2. Chen,X. (2012) Small RNAs in development - insights from plants. *Curr. Opin. Genet. Dev.*, **22**, 361–367.
3. Pantaleo,V. (2011) Plant RNA silencing in viral defence. *Adv. Exp. Med. Biol.*, **722**, 39–58.
4. Mlotshwa,S., Pruss,G.J. and Vance,V. (2008) Small RNAs in viral infection and host defense. *Trends Plant Sci.*, **13**, 375–382.
5. Burgyan,J. and Havelda,Z. (2011) Viral suppressors of RNA silencing. *Trends Plant Sci.*, **16**, 265–272.
6. Mallory,A. and Vaucheret,H. (2010) Form, function, and regulation of ARGONAUTE proteins. *Plant Cell*, **22**, 3879–3889.
7. Vaucheret,H. (2009) AGO1 homeostasis involves differential production of 21-nt and 22-nt miR168 species by MIR168a and MIR168b. *PLoS One*, **4**, e6442.
8. Vaucheret,H., Vazquez,F., Crete,P. and Bartel,D.P. (2004) The action of ARGONAUTE1 in the miRNA pathway and its regulation by the miRNA pathway are crucial for plant development. *Genes Dev.*, **18**, 1187–1197.
9. Vaucheret,H., Mallory,A.C. and Bartel,D.P. (2006) AGO1 homeostasis entails coexpression of MIR168 and AGO1 and preferential stabilization of miR168 by AGO1. *Mol. Cell*, **22**, 129–136.
10. Varallyay,E., Valoczi,A., Agyi,A., Burgyan,J. and Havelda,Z. (2010) Plant virus-mediated induction of miR168 is associated with repression of ARGONAUTE1 accumulation. *EMBO J.*, **29**, 3507–3519.
11. Silhavy,D., Molnar,A., Lucioli,A., Szittya,G., Hornyik,C., Tavazza,M. and Burgyan,J. (2002) A viral protein suppresses RNA silencing and binds silencing-generated, 21- to 25-nucleotide double-stranded RNAs. *EMBO J.*, **21**, 3070–3080.
12. Lakatos,L., Szittya,G., Silhavy,D. and Burgyan,J. (2004) Molecular mechanism of RNA silencing suppression mediated by p19 protein of tombusviruses. *EMBO J.*, **23**, 876–884.
13. Varallyay,E. and Havelda,Z. (2013) Unrelated viral suppressors of RNA silencing mediate the control of ARGONAUTE1 level. *Mol. Plant Pathol.*, **14**, 567–575.
14. Dalmay,T., Rubino,L., Burgyan,J., Kollar,A. and Russo,M. (1993) Functional analysis of cymbidium ringspot virus genome. *Virology*, **194**, 697–704.
15. Burgyan,J., Rubino,L. and Russo,M. (1996) The 5'-terminal region of a tombusvirus genome determines the origin of multivesicular bodies. *J. Gen. Virol.*, **77**(Pt 8), 1967–1974.
16. Csorba,T. and Burgyan,J. (2011) Gel mobility shift assays for RNA binding viral RNAi suppressors. *Methods Mol. Biol.*, **721**, 245–252.
17. Vargason,J.M., Szittya,G., Burgyan,J. and Tanaka Hall,T.M. (2003) Size selective recognition of siRNA by an RNA silencing suppressor. *Cell*, **115**, 799–811.
18. Varallyay,E., Burgyan,J. and Havelda,Z. (2008) MicroRNA detection by northern blotting using locked nucleic acid probes. *Nat. Protoc.*, **3**, 190–196.
19. Csorba,T., Bovi,A., Dalmay,T. and Burgyan,J. (2007) The p122 subunit of Tobacco Mosaic Virus replicase is a potent silencing suppressor and compromises both small interfering RNA- and microRNA-mediated pathways. *J. Virol.*, **81**, 11768–11780.
20. Ye,K., Malinina,L. and Patel,D.J. (2003) Recognition of small interfering RNA by a viral suppressor of RNA silencing. *Nature*, **426**, 874–878.
21. Omarov,R., Sparks,K., Smith,L., Zindovic,J. and Scholthof,H.B. (2006) Biological relevance of a stable biochemical interaction between the tombusvirus-encoded P19 and short interfering RNAs. *J. Virol.*, **80**, 3000–3008.
22. Szittya,G., Silhavy,D., Molnar,A., Havelda,Z., Lovas,A., Lakatos,L., Banfalvi,Z. and Burgyan,J. (2003) Low temperature inhibits RNA silencing-mediated defence by the control of siRNA generation. *EMBO J.*, **22**, 633–640.
23. Scholthof,H.B., Alvarado,V.Y., Vega-Arreguin,J.C., Ciomperlik,J., Odokonyero,D., Brosseau,C., Jaubert,M., Zamora,A. and Moffett,P. (2011) Identification of an ARGONAUTE for antiviral RNA silencing in *Nicotiana benthamiana*. *Plant Physiol.*, **156**, 1548–1555.
24. Burgyan,J., Hornyik,C., Szittya,G., Silhavy,D. and Bisztray,G. (2000) The ORF1 products of tombusviruses play a crucial role in lethal necrosis of virus-infected plants. *J. Virol.*, **74**, 10873–10881.
25. Qu,F. and Morris,T.J. (2002) Efficient infection of *Nicotiana benthamiana* by Tomato bushy stunt virus is facilitated by the coat protein and maintained by p19 through suppression of gene silencing. *Mol. Plant Microbe. Interact.*, **15**, 193–202.
26. Szittya,G., Molnar,A., Silhavy,D., Hornyik,C. and Burgyan,J. (2002) Short defective interfering RNAs of tombusviruses are not

targeted but trigger post-transcriptional gene silencing against their helper virus. *Plant Cell*, **14**, 359–372.
27. Simon,A.E., Roossinck,M.J. and Havelda,Z. (2004) Plant virus satellite and defective interfering RNAs: new paradigms for a new century. *Annu. Rev. Phytopathol.*, **42**, 415–437.
28. Havelda,Z., Hornyik,C., Valoczi,A. and Burgyan,J. (2005) Defective interfering RNA hinders the activity of a tombusvirus-encoded posttranscriptional gene silencing suppressor. *J. Virol.*, **79**, 450–457.
29. Herr,A.J. and Baulcombe,D.C. (2004) RNA silencing pathways in plants. *Cold Spring Harb. Symp. Quant. Biol.*, **69**, 363–370.
30. Szittya,G. and Burgyan,J. (2013) RNA interference-mediated intrinsic antiviral immunity in plants. *Curr. Top Microbiol. Immunol.*, **371**, 153–181.
31. Incarbone,M. and Dunoyer,P. (2013) RNA silencing and its suppression: novel insights from in planta analyses. *Trends Plant Sci.*, **18**, 382–392.
32. Zhang,X., Yuan,Y.R., Pei,Y., Lin,S.S., Tuschl,T., Patel,D.J. and Chua,N.H. (2006) Cucumber mosaic virus-encoded 2b suppressor inhibits Arabidopsis Argonaute1 cleavage activity to counter plant defense. *Genes Dev.*, **20**, 3255–3268.
33. Csorba,T., Lozsa,R., Hutvagner,G. and Burgyan,J. (2010) Polerovirus protein P0 prevents the assembly of small RNA-containing RISC complexes and leads to degradation of ARGONAUTE1. *Plant J.*, **62**, 463–472.
34. Morel,J.B., Godon,C., Mourrain,P., Beclin,C., Boutet,S., Feuerbach,F., Proux,F. and Vaucheret,H. (2002) Fertile hypomorphic ARGONAUTE (ago1) mutants impaired in post-transcriptional gene silencing and virus resistance. *Plant Cell*, **14**, 629–639.
35. Qu,F., Ye,X. and Morris,T.J. (2008) Arabidopsis DRB4, AGO1, AGO7, and RDR6 participate in a DCL4-initiated antiviral RNA silencing pathway negatively regulated by DCL1. *Proc. Natl Acad. Sci. USA*, **105**, 14732–14737.
36. Lang,Q., Jin,C., Lai,L., Feng,J., Chen,S. and Chen,J. (2011) Tobacco microRNAs prediction and their expression infected with Cucumber mosaic virus and Potato virus X. *Mol. Biol. Rep.*, **38**, 1523–1531.
37. Havelda,Z., Varallyay,E., Valoczi,A. and Burgyan,J. (2008) Plant virus infection-induced persistent host gene downregulation in systemically infected leaves. *Plant J.*, **55**, 278–288.
38. Scholthof,H.B. (2006) The Tombusvirus-encoded P19: from irrelevance to elegance. *Nat. Rev. Microbiol.*, **4**, 405–411.
39. Hsieh,Y.C., Omarov,R.T. and Scholthof,H.B. (2009) Diverse and newly recognized effects associated with short interfering RNA binding site modifications on the Tomato bushy stunt virus p19 silencing suppressor. *J. Virol.*, **83**, 2188–2200.
40. Shivaprasad,P.V., Chen,H.M., Patel,K., Bond,D.M., Santos,B.A. and Baulcombe,D.C. (2012) A microRNA superfamily regulates nucleotide binding site-leucine-rich repeats and other mRNAs. *Plant Cell*, **24**, 859–874.
41. Ahn,J.W., Lee,J.S., Davarpanah,S.J., Jeon,J.H., Park,Y.I., Liu,J.R. and Jeong,W.J. (2011) Host-dependent suppression of RNA silencing mediated by the viral suppressor p19 in potato. *Planta*, **234**, 1065–1072.